On the Robustness of Decision-Feedback Detection of DPSK and Differential Unitary Space-Time Modulation in Rayleigh-Fading Channels

Bijoy Bhukania and Philip Schniter
Dept. of Electrical Engineering
The Ohio State University
Columbus, OH 43210
Email: {bhukanib, schniter}@ee.eng.ohio-state.edu

***Abstract*— Decision-feedback differential detection (DFDD) of differential phase-shift keying (DPSK) and differential unitary space-time modulation (DUST) in Rayleigh fading channels exhibits significant performance improvement over standard single-symbol ML detector, but it requires the knowledge of fading correlation and SNR at the receiver. In this paper, we investigate the robustness of the DFDD to imperfect knowledge of fading correlation and SNR. We derive the exact and Chernoff bound expressions for pair-wise word-error probability (PWEP), and then use them to approximate the BER, finding close agreement with simulation results. The relationships between performance and various system parameters, e.g., DFDD length and Doppler mismatch, are also explored.**

I. Introduction

Single antenna differential phase shift keying (DPSK) and its multiple antenna extension, differential unitary space-time modulation (DUST) [1], [2], are used in systems where channel is flat, slow fading and is unknown to the receiver as well as the transmitter. In a fast-fading channel, however, both DUST and DPSK with standard single-symbol ML detection succumb to an error floor when the error due to channel variation dominates that due to additive noise [3]–[5]. Decision-feedback differential detection (DFDD) [5]–[7] has been proposed to reduce, and asymptotically eliminate, the error floor and thereby improve the detection performance significantly. DFDD, however, requires the knowledge of channel fading correlation and SNR at the receiver.

Since perfect knowledge of fading correlation and SNR at the receiver is unlikely in practice, especially in scenarios where channel statistics change with time, we analyze the robustness of DFDD to imperfect parameter knowledge. Relative to the *actual* fading correlation and SNR, we define the *assumed* fading correlation and SNR, and consider DFDD operation in accordance with the *assumed* parameters. Under such conditions, we derive exact and Chernoff bound expressions for PWEP and later use them to approximate the BER, resulting in close agreement with the simulation results. In addition, we analyze the "equivalent SNR loss" due to parameter mismatch. The results presented in this paper are applicable to both DUST and DPSK.

Notations: $\mathbf{I}_P$ denotes identity matrix of size $P \times P$. The operator vec$(\cdot)$, e.g., $\mathbf{x}_n = \text{vec}(X_n)$, denotes stacking of the columns of matrix X_n in column vector $\mathbf{x}_n$. $(\cdot)^*$ denotes conjugate transposition, $\otimes$ denotes the Kronecker product, tr$(\cdot)$ denotes the trace operator, det$(\cdot)$ the determinant, and $\Re(\cdot)$ the extraction of the real valued component. $\prod_{j=k_l}^{k_u} A_j = A_{k_l} A_{k_l+1} \cdots A_{k_u}$ if $k_u \geq k_l$, otherwise it denotes identity matrix of appropriate size.

II. System model

We consider the system model

$$X_n = \sqrt{\tfrac{\rho}{M}} S_n H_n + W_n \tag{1}$$

where X_n is the $M \times P$ received matrix during the n^{th} matrix-symbol interval, and where M and P are the number of transmit and receive antennas, respectively. H_n is the $M \times P$ MIMO channel response matrix during the n^{th} matrix-symbol interval, containing i.i.d. unit variance proper complex Gaussian entries. S_n is the n^{th} $M \times M$ transmitted matrix-symbol, encoded as $S_n = V_{z_n} S_{n-1}$. $z_n \in \mathcal{L} = \{0, 1, \ldots, 2^{\eta M} - 1\}$ is the time-n integer index into matrix alphabet $\mathcal{A}$ of size $2^{\eta M}$, so that $V_{z_n} \in \mathcal{A}$. Thus η is the number of bits per channel use. S_n and V_{z_n} are unitary for all n, W_n is a matrix of i.i.d. unit variance proper complex Gaussian entries, and ρ is the average SNR per receive antenna.

Note that the system model (1) assumes that the channel H_n is fixed for M signaling intervals within the n^{th} matrix-symbol interval, i.e., the channel is block-fading. However, for the special case of diagonal codes, (1) can be shown to be a valid system model even in a continuous fading channel such that the k^{th} row of H_n is the k^{th} row of $H_{k,n}$, where $H_{k,n}$ is the MIMO channel response matrix at the k^{th} time instant within the n^{th} matrix-symbol interval, i.e., at the $(nM+k)^{th}$ channel use [8]. Note that, if the MIMO fading process $H_{k,n}$ is independent between antennas, then H_n is also independent between antennas, and that (1) is an approximate model when non-diagonal constellations are used in continuous fading.

III. Decision-Feedback Differential Detection

DFDD can be derived in two ways. Using m-DFDD to denote DFDD that employs $m-1$ past decisions for improved

detection performance, m-DFDD can be derived from the m-symbol ML differential detection rule [4], [8] by setting the the past $m-1$ symbols equal to their previously-detected values. For DUST, m-DFDD takes the form [7]

$$\hat{z}_n = \arg\max_{z_n \in \mathcal{L}} \Re\left[\mathrm{tr}\left\{\sum_{k=0}^{m-1} a_{0,k+1}^{(m)} X_n^* \mathcal{V}_n^k X_{n-k-1}\right\}\right] \quad (2)$$

where $\mathcal{V}_n^k = V_{z_n}\prod_{j=1}^{k} V_{\hat{z}_{n-j}}$ such that $\{\hat{z}_k\}_{k=n-m+1}^{n-1}$ are the previously detected symbols, and the coefficient $a_{i,j}^{(m)}$ can be found at the i^{th} row and j^{th} column of $-T^{(m)^{-1}}$:

$$T^{(m)} = \mathbf{I}_{m+1} + \frac{\rho}{M}\begin{bmatrix} \zeta_0 & \cdots & \zeta_m \\ \vdots & \ddots & \vdots \\ \zeta_m^* & \cdots & \zeta_0 \end{bmatrix} \quad (3)$$

In (3), ζ_k is defined such that $\mathrm{E}[\mathbf{h}_n\mathbf{h}_{n-k}^*] = \zeta_k\mathbf{I}_{MP}$ for $\mathbf{h}_k = \mathrm{vec}(H_k)$.

DFDD can also be derived from quasi-coherent detection based on MMSE channel prediction. Here we present a summary of the derivations in [7]. Assuming for the moment that both $\{X_k\}_{k=n-m}^{n-1}$ and $\{S_k\}_{k=n-m}^{n-1}$ are known, the MMSE estimate of $\mathbf{h}_n$ is given in terms of $\mathbf{x}_n = \mathrm{vec}(X_n)$ as

$$\hat{\mathbf{h}}_n = B^*\underline{\mathbf{x}}_{n-1},\ \underline{\mathbf{x}}_{n-1} = \left[\mathbf{x}_{n-1}^* \cdots \mathbf{x}_{n-m}^*\right]^* \quad (4)$$

$$B = \sqrt{\frac{\rho}{M}}\mathcal{S}_{n-1}\left((T^{(m-1)^{-1}}\mathbf{g}) \otimes \mathbf{I}_{MP}\right) \quad (5)$$

$$\mathbf{g} = [\zeta_1\ \zeta_2\ \ldots\ \zeta_m]^*$$

$$\mathcal{S}_{n-1} = \begin{bmatrix} \overline{S}_{n-1} & \mathbf{0} & \mathbf{0} \\ & \ddots & \vdots \\ \mathbf{0} & \cdots & \overline{S}_{n-m} \end{bmatrix},\ \overline{S}_k = \mathbf{I}_P \otimes S_k$$

which can be simplified to yield

$$\hat{H}_n = \xi\sum_{k=0}^{m-1} a_{0,k+1}^{(m)} S_{n-k-1}^* X_{n-k-1} \quad (6)$$

where $\xi = \left(\sqrt{M/\rho} + \sqrt{\rho/M}(1-\rho/M\mathbf{g}^* T^{(m-1)^{-1}}\mathbf{g})\right)$. Writing $\mathbf{h}_n = \hat{\mathbf{h}}_n + \tilde{\mathbf{h}}_n$, it can be shown that

$$\mathbf{x}_n = \sqrt{\tfrac{\rho}{M}}\left(\mathbf{I}_P \otimes S_n\right)\hat{\mathbf{h}}_n + \underbrace{\sqrt{\tfrac{\rho}{M}}\left(\mathbf{I}_P \otimes S_n\right)\tilde{\mathbf{h}}_n + \mathbf{w}_n}_{\tilde{\mathbf{w}}_n} \quad (7)$$

where $\mathbf{w}_n = \mathrm{vec}(W_n)$. Since it can also be shown that $\mathrm{E}[\tilde{\mathbf{w}}_n\tilde{\mathbf{w}}_n^*] = \sigma_{\tilde{W}}^2\mathbf{I}_{MP}$ and $\mathrm{E}[\hat{\mathbf{h}}_n\tilde{\mathbf{w}}_n^*] = \mathbf{0}$, (7) implies that the ML detection of z_n given known $(\mathbf{I}_P \otimes S_{n-1})\hat{\mathbf{h}}_n$ can be accomplished via

$$\hat{z}_n = \arg\min_{z_n \in \mathcal{L}} \|\mathbf{x}_n - \sqrt{\tfrac{\rho}{M}}(\mathbf{I}_P \otimes V_{z_n})(\mathbf{I}_P \otimes S_{n-1})\hat{\mathbf{h}}_n\|^2 \quad (8)$$

Under the assumption of correct past decisions, i.e., $\hat{z}_k = z_k, k = n-m+1, \ldots, n-1$, it is possible to verify that (8) is, in fact, equivalent to (2).

It is important to note from (6) that, while computation of $\hat{H}_n$ requires knowledge of the (unknown) transmitted symbols $\{S_k\}_{k=n-m}^{n-1}$, computation of $(\mathbf{I}_P \otimes S_{n-1})\hat{\mathbf{h}}_n = \mathrm{vec}(S_{n-1}\hat{H}_n)$ requires only the past information symbols $\{V_{z_k}\}_{k=n-m+1}^{n-1}$, allowing quasi-coherent detection of V_{z_n} using (2) or (8) via the error-free past decisions $\{\hat{V}_{z_k}\}_{k=n-m+1}^{n-1}$. In practice, of course, the past decisions might contain errors, leading to suboptimal performance (and possibly error propagation).

From (6), we see that the channel estimator embedded in the m-DFDD can be described as a filter with impulse response $\{a_{0,k}^{(m)}\}_{k=1}^{m}$, input $Y_k = S_k^* X_k = \sqrt{\frac{\rho}{M}}H_k + S_k^* W_k$, and output $\hat{H}_k$. Recall that $\{H_k\}$, the response of a fading channel, is typically a lowpass random process whose bandwidth is defined by the Doppler spread of the channel [11]. Therefore, the filter acts to attenuate the wideband additive noise $S_k^* W_k$ and predict the desired process.

The passband width of the optimal linear predictor will be commensurate with the desired-process bandwidth in the presence of noise and will shrink as the noise power increases and expand as noise power decreases. Thus the effect of under-estimating the Doppler spread can be somewhat countered by overestimating the SNR ρ and vice versa. However, simultaneous over (or under) estimation of both Doppler spread and SNR can result in severe performance degradation. Note that the excess prediction error due to over-estimation of Doppler frequency is directly proportional to noise power, and therefore becomes asymptotically negligible as SNR increases. On the other hand, error due to under-estimation of Doppler frequency does not decrease with increasing SNR, and so the estimation error succumbs to a floor. Note that, when the prediction filter length m is small and the receiver under-estimates the Doppler spread, the performance degradation is small since the filter has a wide "transition band". On the other hand, larger m allows a sharper transition band and hence reduces robustness to Doppler mismatch. These notions are confirmed by the numerical results in Sections IV & V.

IV. Error Performance

We have seen that m-DFDD requires knowledge of the SNR ρ—henceforth termed "coherent SNR" * — and the fading correlations $\{\zeta_k\}_{k=0}^{m}$. In this section, we derive exact and Chernoff bound expressions for PWEP when the receiver has imperfect knowledge of fading correlations and SNR ρ and then use them to approximate the BER.

A. Exact PWEP

We consider the case where the receiver operates under the knowledge of assumed "coherent SNR" and fading correlation. Relative to the *actual* coherent SNR ρ, we introduce the *assumed* coherent SNR ρ_a. Similarly, we construct the assumed matrices $T_a^{(m)}$, $\mathbf{g}_a$, and B_a corresponding to $T^{(m)}$, $\mathbf{g}$ and B defined in Section III. Thus, the linear estimator is $B_a = \sqrt{\rho_a/M}\mathcal{S}_{n-1}\left((T_a^{(m-1)^{-1}}\mathbf{g}_a) \otimes \mathbf{I}_{MP}\right)$ and the channel estimate is $\hat{\mathbf{h}}_n = B_a^*\underline{\mathbf{x}}_{n-1}$, and $\tilde{\mathbf{h}}_n = \mathbf{h}_n - B_a^*\underline{\mathbf{x}}_{n-1}$, $\tilde{\mathbf{w}}_n = \sqrt{\frac{\rho}{M}}(\mathbf{I}_P \otimes S_n)\tilde{\mathbf{h}}_n + \mathbf{w}_n$.

Using $\underline{\mathbf{x}}_{n-1} = \sqrt{\frac{\rho}{M}}\mathcal{S}_{n-1}\underline{\mathbf{h}}_{n-1} + \underline{\mathbf{w}}_{n-1}$, $E[\underline{\mathbf{x}}_{n-1}\underline{\mathbf{x}}_{n-1}^*] = \mathcal{S}_{n-1}\left(T^{(m-1)} \otimes \mathbf{I}_{MP}\right)\mathcal{S}_{n-1}$, and $E[\underline{\mathbf{h}}_{n-1}\mathbf{h}_n^*] = \mathbf{g} \otimes \mathbf{I}_{MP}$, where $\underline{\mathbf{h}}_{n-1} = \left[\mathbf{h}_{n-1}^* \cdots \mathbf{h}_{n-m}^*\right]^*$, $\underline{\mathbf{w}}_{n-1} = \left[\mathbf{w}_{n-1}^* \cdots \mathbf{w}_{n-m}^*\right]^*$, we have shown that, $E[\hat{\mathbf{h}}_n\hat{\mathbf{h}}_n^*] = \hat{\sigma}_h^2\mathbf{I}_{MP}$, $E[\tilde{\mathbf{w}}_n\tilde{\mathbf{w}}_n^*] =$

* Since ρ is the true SNR under perfect channel state information.

$\tilde{\sigma}_w^2 \mathbf{I}_{MP}$, and $E[\tilde{\mathbf{w}}_n \hat{\mathbf{h}}_n^* (\mathbf{I}_P \otimes S_{n-1}^*)] = \sigma_{wh}^2 (\mathbf{I}_P \otimes V_{z_n})$, where [8]

$$\hat{\sigma}_h^2 = \tfrac{\rho_a}{M} \left(\mathbf{g}_a^* T_a^{(m-1)^{-1}} T^{(m-1)} T_a^{(m-1)^{-1}} \mathbf{g}_a \right) \quad (9)$$

$$\tilde{\sigma}_w^2 = (\tfrac{\rho}{M} + 1) - \tfrac{2\sqrt{\rho^3 \rho_a}}{M^2} \Re(\mathbf{g}^* T_a^{(m-1)^{-1}} \mathbf{g}_a) + \tfrac{\rho}{M} \hat{\sigma}_h^2$$

$$\sigma_{wh}^2 = \sqrt{\tfrac{\rho}{M}} \left(\tfrac{\sqrt{\rho \rho_a}}{M} (\mathbf{g}^* T_a^{(m-1)^{-1}} \mathbf{g}_a) - \hat{\sigma}_h^2 \right) \quad (10)$$

Now defining $\breve{\mathbf{x}}_n = \mathbf{x}_n / \tilde{\sigma}_w$, $\breve{\mathbf{h}}_n = (\mathbf{I}_P \otimes S_{n-1}) \hat{\mathbf{h}}_n / \hat{\sigma}_h$, $\breve{\mathbf{w}}_n = \tilde{\mathbf{w}}_n / \tilde{\sigma}_w$, and $\breve{\rho} = \rho \hat{\sigma}_h^2 / \tilde{\sigma}_w^2$, we can write (7) as

$$\breve{\mathbf{x}}_n = \sqrt{\tfrac{\breve{\rho}}{M}} (\mathbf{I}_P \otimes V_{z_n}) \breve{\mathbf{h}}_n + \breve{\mathbf{w}}_n \quad (11)$$

such that $E[\breve{\mathbf{h}}_n \breve{\mathbf{h}}_n^*] = E[\breve{\mathbf{w}}_n \breve{\mathbf{w}}_n^*] = \mathbf{I}_{MP}$ and $E[\breve{\mathbf{w}}_n \breve{\mathbf{h}}_n^*] = \frac{\sigma_{wh}^2}{\hat{\sigma}_h \tilde{\sigma}_w} \mathbf{I}_P \otimes V_{z_n}$.

Given the the symbol V_1 was sent, the receiver will detect V_2, and thus make a decision error, if

$$\|\breve{\mathbf{x}}_n - \sqrt{\tfrac{\breve{\rho}}{M}} (\mathbf{I}_P \otimes V_2) \breve{\mathbf{h}}_n\|^2 < \|\breve{\mathbf{x}}_n - \sqrt{\tfrac{\breve{\rho}}{M}} (\mathbf{I}_P \otimes V_1) \breve{\mathbf{h}}_n\|^2$$

$$\iff Q = [\mathbf{y}_1^* \ \mathbf{y}_2^*] \underbrace{\begin{bmatrix} \mathbf{I}_{MP} & \mathbf{0} \\ \mathbf{0} & -\mathbf{I}_{MP} \end{bmatrix}}_{K} \underbrace{\begin{bmatrix} \mathbf{y}_1 \\ \mathbf{y}_2 \end{bmatrix}}_{\mathbf{y}} < 0 \quad (12)$$

where $\mathbf{y}_1 = \sqrt{\tfrac{\breve{\rho}}{M}} (\mathbf{I}_P \otimes (V_1 - V_2)) \breve{\mathbf{h}}_n + \breve{\mathbf{w}}_n$ and $\mathbf{y}_2 = \breve{\mathbf{w}}_n$, and the PWEP $P_{1,2} = \Pr(V_1 \to V_2)$ is given by [9]

$$P_{1,2} = \Pr(Q \le 0) = \sum_{\substack{\text{poles } \omega = jp \\ p > 0}} \text{Res} \left[-\frac{\Phi_Q(\omega)}{\omega} \right] \quad (13)$$

where the summation is taken over the poles in the upper half plane (UHP) and $\Phi_Q(\omega) = E[e^{j\omega Q}]$. The characteristic function of Q, a Hermitian quadratic of Gaussian vector, is given by (for proof, see Appendix-A.9 in [8])

$$\Phi_Q(\omega) = \prod_{k=1}^{M} \left[\frac{\breve{\rho} \sigma_k^2}{M} (1 - \tau^2)(\omega - j p_k^+)(\omega - j p_k^-) \right]^{-P} \quad (14)$$

$$p_k^{\pm} = \tfrac{1}{2 b_k} \left[a_k \pm \sqrt{a_k^2 + 4 b_k} \right] \quad (15)$$

$$a_k = (\tfrac{\breve{\rho}}{M} + \tau \sqrt{\tfrac{\breve{\rho}}{M}}) \sigma_k^2, \ \ b_k = \tfrac{\breve{\rho} \sigma_k^2}{M} (1 - \tau^2)$$

where σ_k is the k^{th} singular value of $V_1 - V_2$ and $\tau = \frac{\sigma_{wh}^2}{\hat{\sigma}_h \tilde{\sigma}_w}$. Note that the characteristic function $\Phi_Q(\omega)$, and hence the PWEP, depend on the signal only through the singular values of $V_1 - V_2$. Since the singular values of $V_1 - V_2$ and $\mathbf{I}_M - V_2 V_1^*$ are the same, $\Pr(V_1 \to V_2) = \Pr(\mathbf{I}_M \to V_2 V_1^*)$.

Computation of the PWEP using (13) involves taking residues at poles with multiplicities greater than 1, which can be complicated. A simple method to evaluate the PWEP in such cases has been proposed in [10], where the poles are perturbed by small amount to eliminate multiplicity, and the PWEP is computed by taking residues at *all* the simple poles in UHP. This method produces an lower bound on the PWEP if all the concerned poles are moved away from origin, and upper bound when moved towards the origin. In this paper, the i^{th} occurrence of p_k^+ is replaced by $\tilde{p}_{(k-1)Pm_k+i}^+ = p_k^+ + (i-1)\epsilon_k$, yielding the set of simple poles $\{\tilde{p}_k^+\}_{k=1}^{MP}$ in UHP, and hence, the PWEP from (13)

$$P_{1,2} \gtrless \sum_{k=1}^{MP} \frac{1}{\tilde{p}_k^+} \left(\prod_{\ell=1}^{M} \frac{M(1-\tau^2)^{-1}}{\breve{\rho} \sigma_\ell^2 (\tilde{p}_k^+ - p_k^-)} \right)^P \prod_{\substack{\ell=1 \\ \ell \ne k}}^{MP} \frac{1}{(\tilde{p}_\ell^+ - \tilde{p}_k^+)} \quad (16)$$

where an upper bound is obtained by choosing $\epsilon_k = -0.0025 \tilde{p}_k^+$, and a lower bound by choosing $\epsilon_k = 0.0025 \tilde{p}_k^+$. Numerical results in Section V confirm that these bounds are very close to each other, and thus this method produces an accurate estimate of the PWEP.

B. Chernoff bound

In order to further analyze the performance loss due to parameter mismatch, we have derived the Chernoff bound on the PWEP:

$$P_{1,2} \le \frac{1}{2} \prod_{k=1}^{M} \left[1 + \frac{\sigma_k^2}{4(1-\tau^2)} \left(\sqrt{\frac{\breve{\rho}}{M}} + \tau \right)^2 \right]^{-P} \quad (17)$$

where $\tau = \frac{\sigma_{wh}^2}{\hat{\sigma}_h \tilde{\sigma}_w}$ (For proof, see Sec. 4.2.4 in [8].).

Observe that the diversity advantage of the system is MP, while the performance is governed by the "equivalent SNR" $(\sqrt{\breve{\rho}/M} + \tau)^2 / (1 - \tau^2)$. The "equivalent SNR" in the absence of mismatch is defined as

$$\breve{\rho}_{\text{perfect}} = \frac{1}{1-\tau^2} \left(\sqrt{\breve{\rho}/M} + \tau \right)^2 \Big|_{\rho_a = \rho, T_a^{(m)} = T^{(m)}, \mathbf{g}_a = \mathbf{g}}$$

To analyze the performance degradation due to parameter mismatch, we define the "equivalent SNR loss" as

$$\alpha = \frac{(\sqrt{\breve{\rho}/M} + \tau)^2}{1 - \tau^2} \frac{1}{\breve{\rho}_{\text{perfect}}} \quad (18)$$

C. Approximate Bit Error Rate

In practice, BER is often more useful than PWEP. Since $\Pr(V_1 \to V_2) = \Pr(\mathbf{I}_M \to V_2 V_1^*)$, $V_1, V_2 \in \mathcal{A} \implies V_2 V_1^* \in \mathcal{A}$, and ηM bits are encoded in each transmitted matrix-symbol, under the assumption of Gray mapping and equal prior probabilities the BER can be written as

$$P_{\text{genie}} \approx \frac{1}{\eta M} \sum_{j=1}^{2^{\eta M} - 1} d(\mathbf{I}_M, V_j) \Pr(\mathbf{I}_M \to V_j) \quad (19)$$

where $d(V_j, V_k)$ is the Hamming distance between the binary representations of V_j and V_k. $P_{\text{genie}}^{\text{Chernoff}}$ is obtained from (19) when the PWEP from (17) is used, and $P_{\text{genie}}^{(L)}$ & $P_{\text{genie}}^{(U)}$ are obtained from (19) when (16) is used.

For realizable m-DFDD, the influence of incorrect past-decisions must be taken into account for $m > 1$. Through numerical evaluation we find that the BER of realizable DFDD is approximately twice that of genie-aided DFDD, since every error is likely to cause another error due to error propagation, which is in accordance with the approximation for DPSK [12].

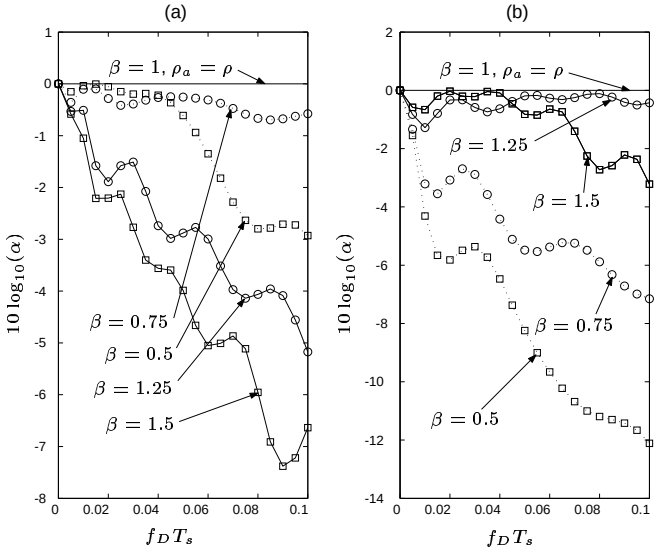

Fig. 1. SNR loss α for $f_D T_s|_a = \beta f_D T_s$, "coherent SNR" $\rho = 20$dB and $\rho_a =$ (a) 30dB, (b) 10dB

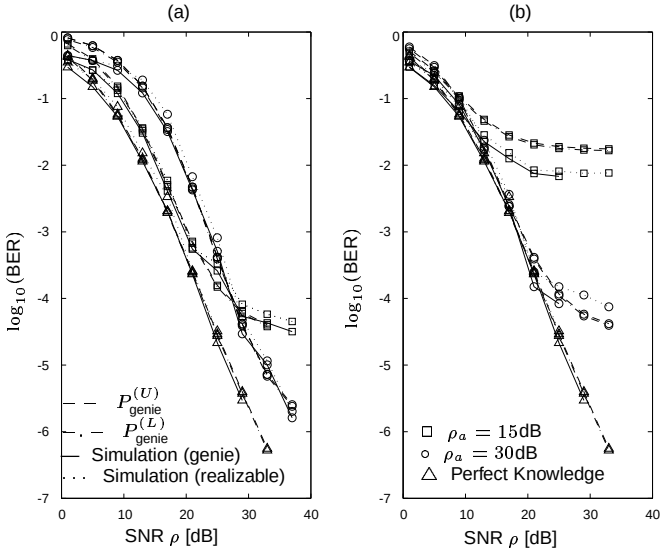

Fig. 2. Genie-aided 6-DFDD in continuous fading with *actual* $f_D T_s = 0.075$ and *assumed* $f_D T_s|_a =$ (a) 0.1, (b) 0.05

V. Simulations & Numerical Results

For numerical examples in this paper, we consider a system with $M = 2$ transmit and $P = 2$ receive antennas and the constellation specified in [1] for $\eta = 1$. The MIMO channel exhibits Rayleigh fading [11] where the correlation between fading coefficients k matrix-symbols apart is given by $\zeta_k = J_0(2\pi f_D T_s M k)$ and where $f_D T_s$ is the normalized Doppler frequency. Observe that $f_D T_s M$ is the effective normalized Doppler frequency for $M \times M$ symbols. Since the performance of the detectors degrades with increasing Doppler frequency [5], [7], increasing M in a fading channel, therefore, may degrade the performance.

A. Equivalent SNR Loss

Fig. 1 shows the variations in equivalent SNR loss α from (18) with respect to the *actual* Doppler frequency $f_D T_s$, when the actual "coherent SNR" is $\rho = 20$dB, the assumed Doppler frequency is $f_D T_s|_a = \beta f_D T_s$, and the assumed "coherent SNR" is $\rho_a = 10, 30$dB. From Fig. 1(a) we find that, when $\rho_a = 30\text{dB} > \rho$, $\beta < 1$, i.e., under-estimating the Doppler frequency results in lower SNR loss compared to the case of $\beta > 1$. Fig. 1(b), where $\rho_a = 10\text{dB} < \rho$, shows the opposite trend. As predicted in Section III and shown in Fig. 1, when $\beta < 1$, performance can be improved by choosing $\rho_a > \rho$ and vice-versa, whereas the performance loss can be significant when $\rho_a < \rho$ and $\beta < 1$, or when $\rho_a > \rho$ and $\beta > 1$.

B. BER in continuous fading

Next we analyze the robustness of the DFDD in continuous-fading channel. Recall that the theoretical analyses in Section IV are applicable when the channel is block-fading, or when the channel is continuously fading under diagonal constellations.

Fig. 2 investigates the analytical and simulated performance of 6-DFDD when the *actual* normalized Doppler frequency is 0.075 and the receiver has imperfect knowledge of $f_D T_s$ and SNR ρ. The performance of the detectors with perfect knowledge of $f_D T_s$ and SNR is compared to the performance of detectors with assumed $f_D T_s|_a = 0.075, 0.05$ and $\rho_a = 15, 30$dB. In all cases, the effect of error propagation is observed through performance difference of genie aided and realizable 6-DFDD. Note that the approximations of the BER, $P^{(U)}_{\text{genie}}$ and $P^{(L)}_{\text{genie}}$ from (19) are very close to each other, and closely follow the simulated BER of genie aided DFDD.

As predicted in Section III and shown in Fig. 2, the 6-DFDD succumbs to an error floor when it underestimates the Doppler frequency and a loss in SNR when it overestimates the Doppler frequency. The compensation of performance loss due to over-estimation (under-estimation) of Doppler frequency by under-estimation (over-estimation) of SNR is also depicted in Fig. 2.

Now we analyze the relation between robustness and DFDD length m. Fig. 3 plots the theoretical BER $P^{(U)}_{\text{genie}}$ of genie-aided m-DFDD versus m when the *actual* normalized Doppler spread is $f_D T_s = 0.075$ and the SNR is $\rho = 20$dB. Observe that the performance loss due to under-estimation of the Doppler spread is severe for large m, as predicted in Section III. While over-estimation of Doppler or under/over-estimation of SNR also results in performance loss, it is less severe, and relatively constant over all values of $m > 2$. Finally, it is observed that m-DFDD is quite robust against parameter mismatch when $m = 2$.

VI. Conclusions

In this paper, we have investigated, via simulation as well as theoretical error performance analysis, the robustness of

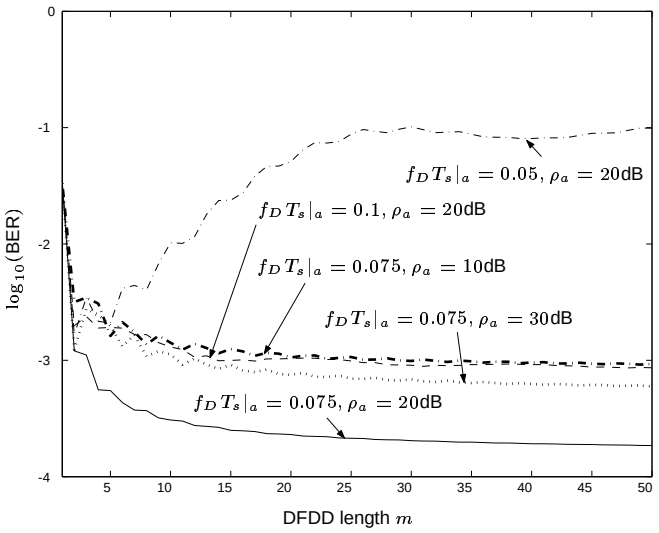

Fig. 3. Genie-aided m-DFDD with $f_D T_s = 0.075$, $\rho = 20$dB

decision-feedback differential detection in Rayleigh fading channels. While underestimation of the Doppler spread results in an error floor, over-estimation results in SNR loss which can be somewhat compensated by underestimating and overestimating the SNR, respectively. Although increasing the DFDD length improves the performance under the assumption of perfect parameter knowledge, the robustness of the DFDD to imperfect parameter knowledge has been shown to decrease with increasing DFDD length.

REFERENCES

[1] B.M. Hochwald and W. Sweldens, "Differential unitary space-time modulation", *IEEE Trans. on Communications*, vol. 48, no. 12, pp. 2041–2052, Dec. 2000.

[2] B.L. Hughes, "Differential space-time modulation", *IEEE Trans. on Information Theory*, vol. 46, no. 7, pp. 2567–2578, Nov. 2000.

[3] C. Peel and A. Swindlehurst, "Performance of unitary space-time modulation in continuously changing channel", in *Proc. IEEE Internat. Conf. on Acoustics, Speech, and Signal Processing*, 2001.

[4] P. Ho and D. Fung, "Error performance of multiple symbol differential detection of PSK signals transmitted over correlated Rayleigh fading channels", *Proc. IEEE Intern. Conf. on Communication*, vol. 2, pp. 568 –574, 1991.

[5] R. Schober, W.H. Gerstacker and J.B. Huber, "Decision feedback differential detection of MDPSK for flat Rayleigh fading channels", *IEEE Trans. on Communications*, vol. 47, no. 7, pp. 1025–1035, July 1999.

[6] R. Schober and H.-J. Lampe, "Noncoherent receivers for differential space-time modulation", *Proc. IEEE Global Telecommunications Conf.*, vol. 2, pp. 1127–1131, 2001.

[7] B. Bhukania and P. Schniter, "Decision-feedback detection of differential unitary space-time modulation in fast Rayleigh-fading channels", in *Proc. Allerton Conf. on Communications, control, and computing*, Oct. 2002.

[8] B. Bhukania, "Detection of differential unitary space-time modulation in fast Rayleigh-fading channels", *M.S. Thesis*, The Ohio State University, Aug. 2002.

[9] J.G. Proakis and M. Salehi, *Communication systems engineering*, Prentice Hall, Inc., New Jersey, 1994.

[10] S. Siwamogsatham, M.P. Fitz and J.H. Grimm, "A new view of performance analysis of transmit diversity schemes in correlated Rayleigh fading", *IEEE Trans. on Information Theory*, vol. 48, no. 4, pp. 950–956, April 2002.

[11] W.C. Jakes, *Microwave Mobile Communications*, IEEE press, Piscataway, NJ, 1993.

[12] F. Edbauer, "Bit error rate of binary and quaternary DPSK signals with multiple differential feedback detection", *IEEE Trans. on Communications*, vol. 40, pp. 457–460, March 1992.